PNAS
www.pnas.org

Supplementary Information for

CHD4 and the NuRD complex directly control cardiac sarcomere formation

Caralynn M. Wilczewski, Austin J. Hepperla, Takashi Shimbo, Lauren Wasson, Zachary L. Robbe, Ian J. Davis, Paul A. Wade, Frank L. Conlon

Frank L. Conlon
Email: frank_conlon@med.unc.edu

This PDF file includes:

Supplementary text
Figs. S1 to S11
Tables S1
Captions for movies S1 to S2
References for SI reference citations

Other supplementary materials for this manuscript include the following:

Movies S1 to S2

www.pnas.org/cgi/doi/10.1073/pnas.1722219115

Materials and Methods

Mice *Chd4*$^{flox/flox}$ mice were obtained from Dr. Katia Georgeopolos(1). *Nkx2-5*$^{Cre/+}$ mice were obtained from Robert Schwartz (2). *Tg(Tnnt2-cre)5Blh*/*JiaoJ* (strain 024240) mice were obtained from JAX. *Chd4* conditional knockout mice and control littermates were obtained by breeding female *Chd4*$^{flox/flox}$ mice to male *Chd4*$^{flox/+}$*;Nkx2-5*$^{Cre/+}$ mice. Research was approved by the Institutional Animal Care and Use Committee at the University of North Carolina and conforms to the Guide for the Care and Use of Laboratory Animals.

Histology and Immunohistochemistry Embryos were fixed in 4% paraformaldehyde/0.1% Tween-20 overnight at 4°C. Embryos were prepared for histology and immunohistochemistry as previously described (3). 10μm paraffin sections were stained with hematoxylin and eosin using standard practices and were imaged on an Olympus BX61 microscope with a Retiga 400R camera. Immunohistochemistry was performed with antigen retrieval on 10μm cryosections as previously described (3) with the following primary antibodies: mouse anti-tropomyosin (DSHB clone CH1), 1:50; rabbit anti-CHD4 (Abcam #ab72418) 1:500; rabbit anti-smooth muscle myosin heavy chain (Abcam ab53219), 1:50; mouse anti-α-actinin (Sigma #A7732), 1:500; rabbit anti-phospho-histone H3 (Millipore #06-570), 1:200. Immunohistochemistry with rabbit anti-troponin I2 (Abcam #ab183508), 1:250; rat anti-PECAM1 (CD31) (BD Biosciences #553370), 1:50 and rabbit anti-cleaved caspase 3 (Cell Signalling #9661), 1:50 did not require antigen retrieval. Secondary antibodies were Alexa Fluor 488 goat anti-mouse IgG H+L (Thermo #A11001), 1:1000; Alexa Fluor 546 goat anti-mouse IgG_1 (Thermo #A21123), 1:1000; Alexa Fluor 647 goat anti-rabbit IgG H+L (Thermo #A21245), 1:1000. Immunohistochemistry images were captured on a Zeiss LSM 700 laser scanning confocal microscope. Whole-mount images were captured using a Leica MZ 16F dissection microscope with a Retiga 4000RV camera. ImageJ (NIH) was used for image analysis and standard image processing.

Image Quantification Thickness of the compact layer was quantified using hematoxylin and eosin stained paraffin with ImageJ on three separate regions per ventricle on three sections (anterior, mid, and posterior heart) per embryo, from three embryos per genotype for total N=243

measurements per genotype. Measurements were averaged separately for each ventricle. Sarcomere organization was quantified by classifying sarcomere structure by α-actinin staining in twenty-five 2μm vectors per field, with three fields per ventricle measured in three embryos per genotype for total N=225 vectors per ventricle per genotype. Statistical comparison between genotypes was performed by χ^2 test.

Z-stacks of smooth muscle myosin heavy chain and α-actinin double-stained sections were deconvolved using AutoQuantX3 software (Media Cybernetics). Fluorescent signals for each channel were measured on 10 vectors per embryo from three embryos per genotype in ImageJ for total N=30 vectors. Correlations between signals were determined using Spearman's rank correlation. Percentage of pHH3 or cleaved caspase 3 positive cardiomyocytes were assessed by counting pHH3 or cleaved caspase 3 positive cells co-stained with tropomyosin from three separate sections per embryo, three independent embryos per genotype for N=9 whole sections counted per genotype. Percentage of PECAM1+/tropomyosin+ cells was calculated by counting PECAM1 positive cells and dividing by tropomyosin positive cells from three separate sections per embryo, three independent embryos per genotype for N=9 whole sections counted per genotype. Statistical comparison between genotypes was performed by Student's t-test except where noted.

Scanning electron microscopy (SEM) A standardized procedure for SEM for the heart was used (3). Briefly, the pericardium was removed before embryos were fixed in 2% paraformaldehyde/2.5% glutaraldehyde in 1X PBS (EM grade, Electron Microscopy Services). Embryos were washed in 1X PBS, dehydrated into 100% ethanol and subject to critical point drying. Dried specimens were mounted ventral side up and ion sputtered with gold palladium to 20nm thickness before scanning with Zeiss Supra 25 FESEM microscope with accelerating voltage of 5000V. SEM photomicrographs were taken in standard orientations and magnifications.

RNA-sequencing and Analysis E10.5 hearts were collected from three *Chd4*$^{flox/flox}$ and three *Chd4*$^{\Delta flox/\Delta flox}$ embryos. E9.5 hearts were collected from five *Chd4*$^{flox/flox}$ and five *Chd4*$^{\Delta flox/\Delta flox}$ embryos. RNA was isolated from individual hearts using standard Trizol extraction. Poly-A selected RNA-seq libraries were prepared at the Vanderbilt Genomic Core using standard library preparation protocols for mRNA. Samples were run on a HiSeq2500 (Illumina) with 50 base-pair single-end reads.

Fastq files were first filtered for reads containing adapter sequences using TagDust (v1.12) (4) with an FDR of 0.001. Reads were then mapped to the mm10 genome using Bowtie (v1.2.0) (5) and options: -m 1, --best, --seed=123, and --nomaqround. Post-alignment, samtools (v1.6) (6) and BedTools (v2.25.0) (7) were used to interconvert and manipulate files. HTSeq (v0.6.2) (8), using the refFlat gtf from UCSC Genome Browser (9), was run to get read counts over genes and these counts were used in DESeq2 (v1.6.3) (10) to determine differential transcripts. Genes with an adjusted p-value < 0.05 and a $\log_2$(Fold Change) > 0.5 in either direction. Gene ontology (GO) terms were analyzed for genes with an adjusted p-value<0.05 using PANTHER (v12.0) Biological Process using Fisher's Exact with FDR multiple test correction (11). Morpheus was used for heatmap visualization (http://software.broadinstitute.org/morpheus/).

Reverse Transcription and Quantitative PCR RNA from individual E10.5 hearts (N=3 per genotype) was isolated using Trizol (Invitrogen) and purified on RNeasy columns (Qiagen). cDNA synthesis was performed using random primers and SuperScript II reverse transcriptase (Invitrogen). Quantitative PCR was performed using the SensiFAST SYBR Hi-ROX Kit (Bioline) with the following primers: Myh11F: GCTAATCCACCCCCGGAGTA, Myh11R: TCGCTGAGCTGCCCTTTCT; Acta1F: GTGACCACAGCTGAACGTG, Acta1R: CCAGGGAGGAGGAAGAGG; Tnnt3F: ACAGATTGGCGGAGGAGAAG, Tnnt3R: CATGGAGGACAGAGCCTTTT; Tnnc2F: GAGATGATCGCTGAGTTCAAG, Tnnc2R: GTCTGCCCTAGCATCCTCAT; Tnni2F: CACCTGAAGAGTGTGATGCTC, Tnni2R: GGGCAGTGTTCTGACAGGTAG; RPS29F: TGGGTCACCAGCAGCTCTAC, RPS29R: GTACTGCCGGAAGCACTGG.

Chromatin Immunoprecipitation (ChIP)-sequencing and Analysis E10.0 hearts from wild-type CD1 mice (thirty hearts per biological replicate, two biological replicates with three technical replicates total) were fixed for chromatin immunoprecipitation as described previously (12). Briefly, hearts were dissected in cold PBS and crosslinked with 1.5mM disuccinimidyl glutarate (Thermo) for 45 minutes at room temperature followed by 1% paraformaldehyde (Electron Microscopy Services) for 10 minutes at room temperature. Fixation was quenched with 125mM glycine. Hearts were washed twice with cold PBS, snap frozen and stored at -80°C. Hearts were prepared for ChIP as described (13) with some modifications. Hearts were resuspended in TD600 buffer (10mM Tris pH7.4, 2mM $MgCl_2$, 600mM NaCl, 1% Triton-100, 0.1% sodium deoxycholate, protease inhibitor (Roche)), dounced 20 times on ice, and sonicated

in a Covaris S220 with the following settings: 145 watts, 20% duty cycle, 200 counts for 1200 seconds at 4°C. Following sonication, samples were centrifuged at 16.1x*g* at 4°C for 5 minutes. The soluble chromatin fraction was diluted 1:4 with TD0 buffer (10mM Tris pH7.4, 2mM $MgCl_2$, 1% Triton-100, 0.1% sodium deoxycholate, 1X protease inhibitor). 10% of the input was stored at -80°C for input library sequencing. 800µl of the chromatin fraction was mixed with 3µg mouse anti-CHD4 antibody (Abcam #ab70469) and rotated overnight at 4°C. 225µg each Protein A and Protein G Dynabeads (Life Technologies) were blocked overnight at 4°C with 2.6µg/µl bovine serum albumin (Jackson Immuno). The next day, blocked beads were rotated with the chromatin immunoprecipitate for 45 minutes at 4°C, then washed three times with SDS-free RIPA buffer (25mM Tris-HCl pH7.4, 150mM NaCl, 1% NP-40, 1% sodium deoxycholate) followed by three washes with high-salt RIPA buffer (25mM Tris-HCl pH7.4, 600mM NaCl, 1% NP-40, 1% sodium deoxycholate), followed by two washes with TM2 buffer (10mM Tris pH7.4, 2mM $MgCl_2$). The beads were prepared for ChIPmentation using the Nextera XT DNA Library Preparation Kit (Illumina) with the following modifications: 10µl Resuspension Buffer, 20µl Tagment DNA Buffer and 10µl Amplicon Tagment Mix with incubation at 37°C for 15 minutes in a thermal cycler (14). Beads were washed with SDS-free RIPA buffer, then incubated in 100µl SDS-free RIPA with 40µg Proteinase K at 65°C for 45 minutes. DNA was purified with Zymo DNA Clean & Concentrator-5 columns (Zymo Research). CHD4 ChIP and input libraries were prepared using the Nextera XT DNA Library Kit and purified using the Agencourt AMPure XP PCR Purification Kit (Beckman Coulter). Libraries were sequenced using the NextSeq 500 at the National Institute of Environmental Health Sciences Epigenomics Core Facility with 36 base pair paired-end reads per sample.

Fastq files were first filtered for reads containing adapter sequences using TagDust (v1.12) (4) with an FDR of 0.001. In-house scripts were used to ensure TagDust filtered reads were maintained in the proper order for alignment. Reads were then mapped to the mm10 genome using Bowtie (v1.2.0) (5) using options: -m 1, --best, --seed=123, --nomaqround. Aligned fragments were then filtered for any duplicate reads based on alignment position using in-house scripts. Samtools (v1.6) (6) and BedTools (v2.25.0) (7) were used to interconvert and manipulate files. Peaks were called with MACS2 (15), and only high confidence peaks (found in at least two of the three replicates) were used in downstream analyses. Cis-regulatory Element Annotation System (CEAS) (v0.9.9.7) (16) was used to assign ChIP-seq peaks to genomic regions after making the mm10 annotation. Gene associations and GO terms for CHD4-bound elements were generated using GREAT (17). Gene tracks were visualized with UCSC Genome Browser (9). Permutations were done using in-house scripts based on the bedtools shuffle tool.

Transmission Electron Microscopy Embryos were collected and fixed in 2% formaldehyde/2.5% glutaraldehyde in 0.15M sodium phosphate buffer, pH 7.4, overnight at 4°C. Following several washes in sodium phosphate buffer, samples were post-fixed for 1 hour in 1% buffered osmium tetroxide, dehydrated through a graded series of ethanol and embedded in PolyBed 812 epoxy resin (Polysciences). Using a diamond knife, 1μm cross-sections were cut, stained with 1% toluidine blue and examined by light microscopy to isolate the area of interest. Ultrasthin sections were cut with a diamond knife (70-80nm thick), mounted on 200 mesh copper grids and stained with 4% aqueous uranyl acetate for 15 minutes followed by Reynolds' lead citrate for 8 minutes (18). The sections were observed using a LEO EM-910 transmission electron microscrope (LEO Electron Microscopy Inc.), accelerating voltage of 80kV and micrographs were taken using a Gatan Orius SC1000 CCD Camera.

Embryonic Echocardiography A pregnant dam carrying *Chd4*$^{flox/flox}$ and *Chd4*$^{\Delta flox/\Delta flox}$ embryos at E10.5 was anesthetized using 1.5% isoflurane and hair was removed from abdomen using topical hair removal agent. The female was placed under a warming lamp and ultrasound gel was applied to the abdomen. Embryos were imaged according to established protocols (19-22). Briefly, embryos were located using the VisualSonics Vevo 2100 Ultrasound machine (Visual Sonics, Inc.) using a 30MHz pediatric probe. B-mode images were used to guide pulsed-wave (PW) Doppler imaging in-line at the point of the atrioventricular canal. Post-imaging, embryos were injected with fluorescent colored microspheres (Cospheric, LLC) diluted in PBS for post-dissection identification and genotyping. Nine cycles of inflow/outflow peaks per recording were measured for peak velocity and velocity time integral (VTI) using VisualSonics image processing software from 5 embryos per genotype for total N=45 measurements per genotype and statistically compared by Student's t-test.

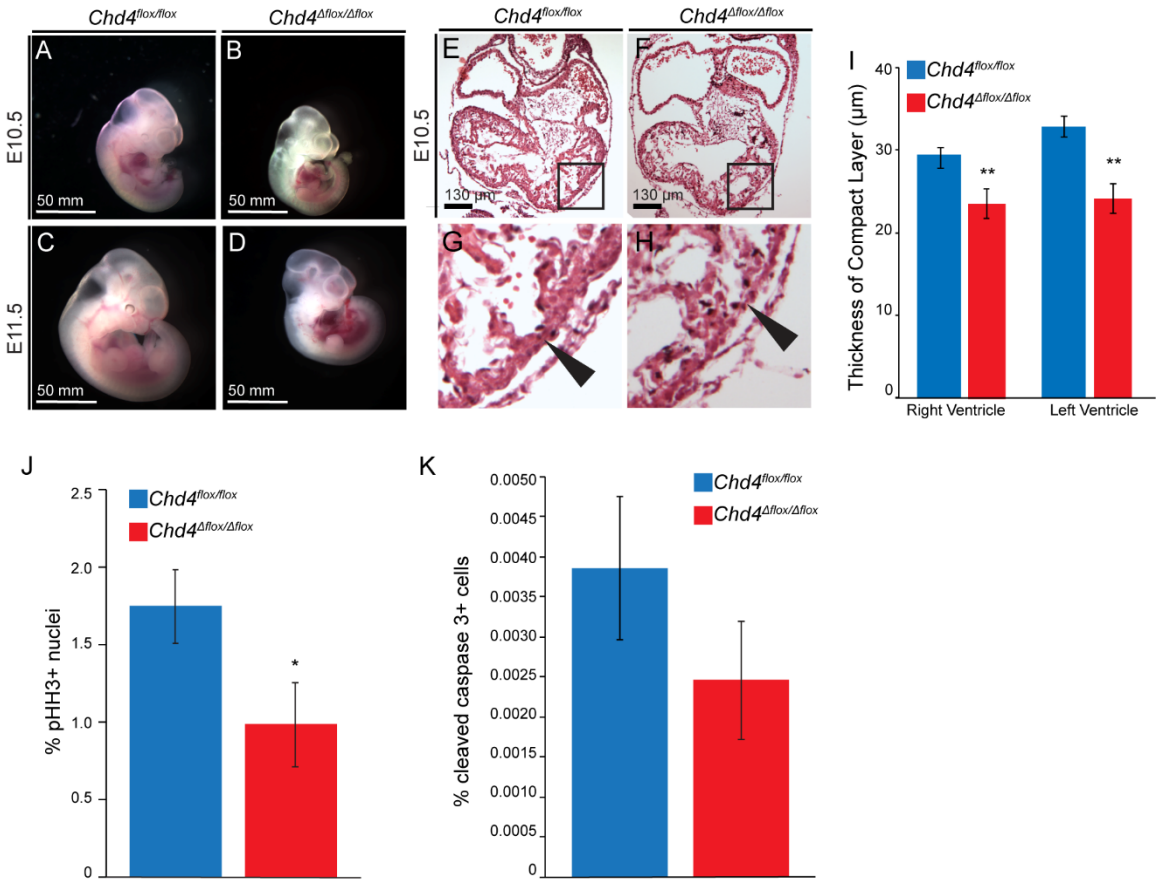

Figure S1. CHD4 is required for myocardial growth before E10.5. (A-D) Gross morphology of *Chd4*$^{\Delta flox/\Delta flox}$ and *Chd4*$^{flox/flox}$ embryos at E10.5 (A,B) and E11.5 (C,D) show growth arrest at E10.5 in the absence of CHD4 in the developing heart with concomitant pericardial edema and hemorrhaging. (E-H) Histological analysis at E10.5 reveals decreased trabecular complexity in the ventriclular myocardium in *Chd4*$^{\Delta flox/\Delta flox}$ hearts (E, F) with a thinner myocardial compact layer compared to *Chd4*$^{flox/flox}$ controls (wedge arrow) (G, H). Boxed area denotes region of higher magnification. (I) Quantification demonstrates significant decrease in thickness of the right and left ventricle compact layer in *Chd4*$^{\Delta flox/\Delta flox}$ compared to *Chd4*$^{flox/flox}$ controls by Student's t-test, N=27 vectors per genotype, error bars represent SEM ± 1.31, 1.27, 1.83, 1.77. (J) Quantification of phosphorylated histone H3+/tropomyosin+ cells indicates a significant decrease in the mitotic index in *Chd4*$^{\Delta flox/\Delta flox}$ hearts by Student's t-test, N=9 sections per genotype, SEM ± 0.238 and 0.271. (J) Quantification of cleaved caspase3+/tropomyosin+ cells indicates no significant change in apoptosis in *Chd4*$^{\Delta flox/\Delta flox}$ hearts by Student's t-test, N=9 sections per genotype, SEM ± 0.0009 and 0.0007. *=p-value<0.05,**=p-value<0.01. oft, outflow tract; lv, left ventricle; la, left atrium; ra, right atrium; rv, right ventricle.

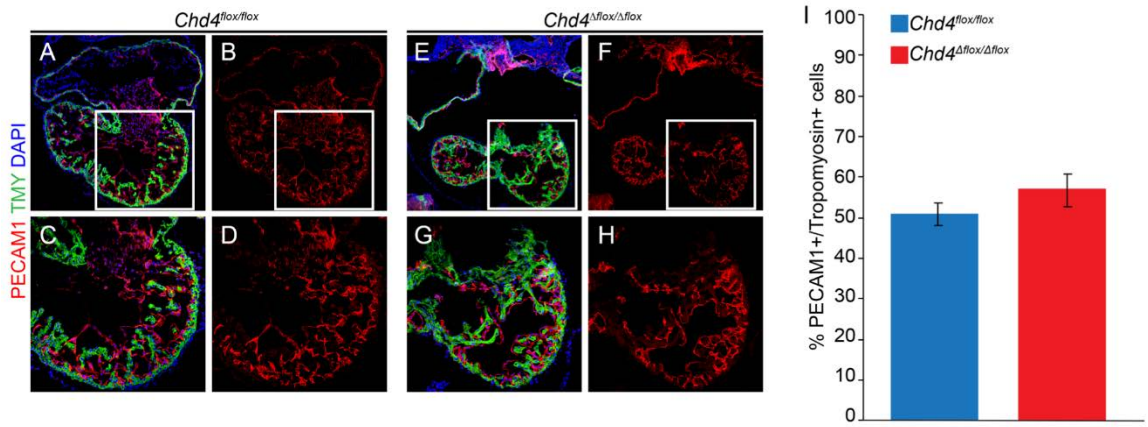

Figure S2. CHD4 ablation does not increase non-cardiomyocyte cell types in the developing heart. (A-H) Platelet endothelial cell adhesion molecule 1 (PECAM1) and tropomyosin (TMY) co-staining followed by quantification of PECAM1+ cells and tropomyosin+ cells (I) demonstrate no significant increase in endothelial cells relative to cardiomyocytes in *Chd4*$^{\Delta flox/\Delta flox}$ embryos compared to control *Chd4*$^{flox/flox}$ embryos at E10.5 by Student's t-test, N=29 regions per genotype, error bars represent SEM ± 0.027 and 0.040. Boxed region denotes area of higher magnification.

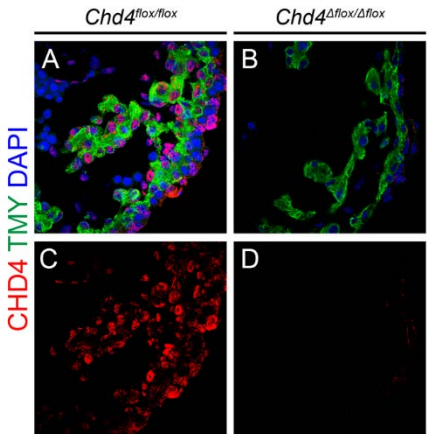

Figure S3. CHD4 is depleted from the myocardium at E9.5. (A-D) CHD4 is depleted from cardiomyocytes costained with tropomyosin (TMY) at E9.5 in *Chd4*$^{\Delta flox/\Delta flox}$ embryos (B,D) compared to *Chd4*$^{flox/flox}$ controls (A,C) after ablation using *Nkx2-5*$^{Cre/+}$.

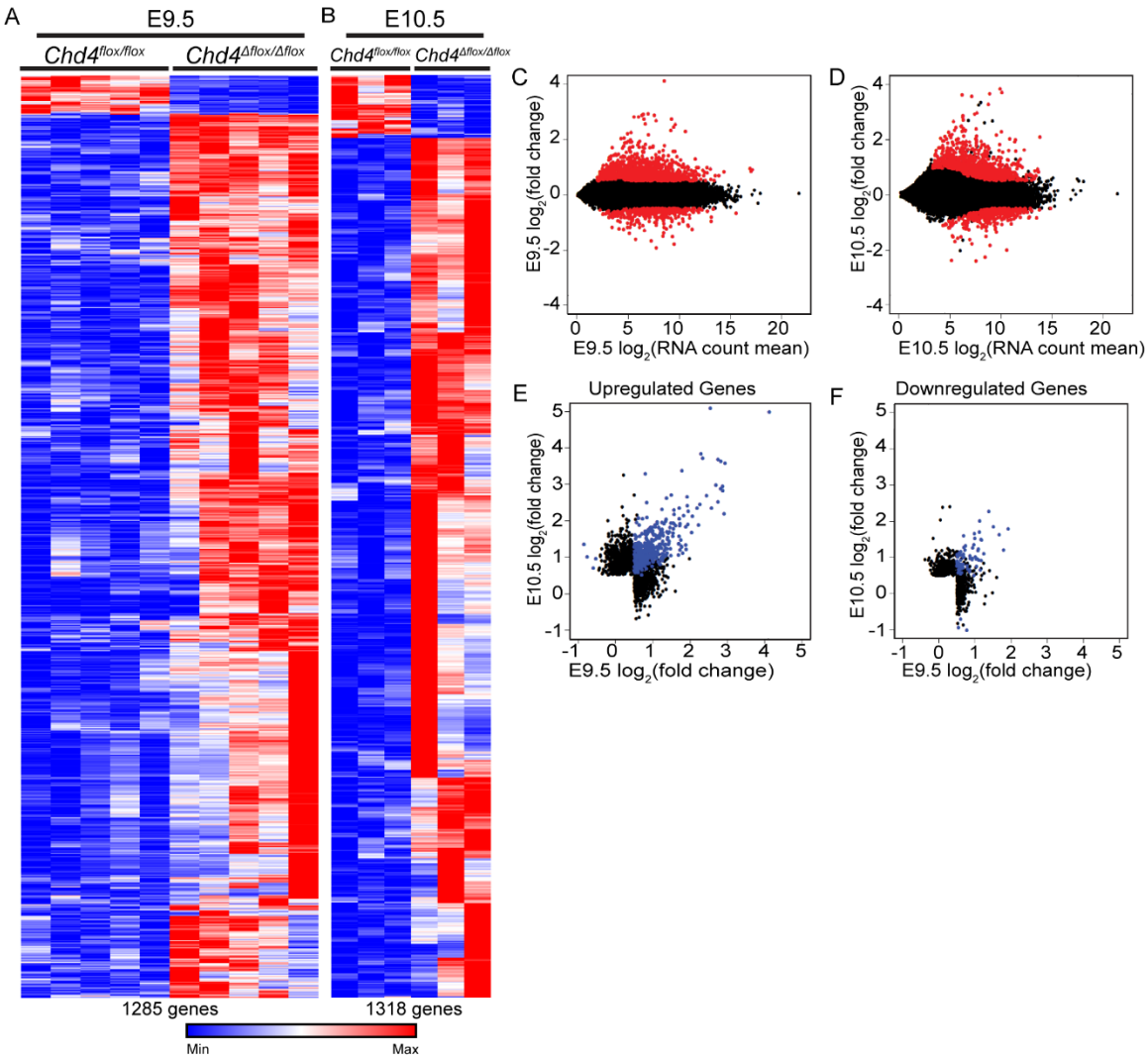

Figure S4. CHD4 temporally restricts gene expression in the developing heart. (A-B) Ward's two-way hierarchical clustering of differential gene expression profiles of E9.5 (A) and E10.5 (B) *Chd4*$^{\Delta flox/\Delta flox}$ and *Chd4*$^{flox/flox}$ hearts show a distinct molecular signature in the absence of CHD4 at both time points. Gene expression is row-scaled to show relative expression. (C-D) MA plots of $\log_2$(fold change) versus $\log_2$(RNA count mean) show a greater number of genes upregulated (913 genes) than downregulated (372 genes) in the absence of CHD4 at E9.5 (C) and a greater number of genes upregulated (920 genes) than downregulated (398 genes) in the absence of CHD4 at E10.5 (D). Red points indicate adjusted p-value of less than 0.05. (E-F) Plotting E10.5 $\log_2$(fold change) versus E9.5 $\log_2$(fold change), with shared upregulated (E) or downregulated (F) genes colored in blue demonstrate distinct requirements in transcriptional regulation dependent on developmental stage. Black points represent genes misexpressed unique to that stage.

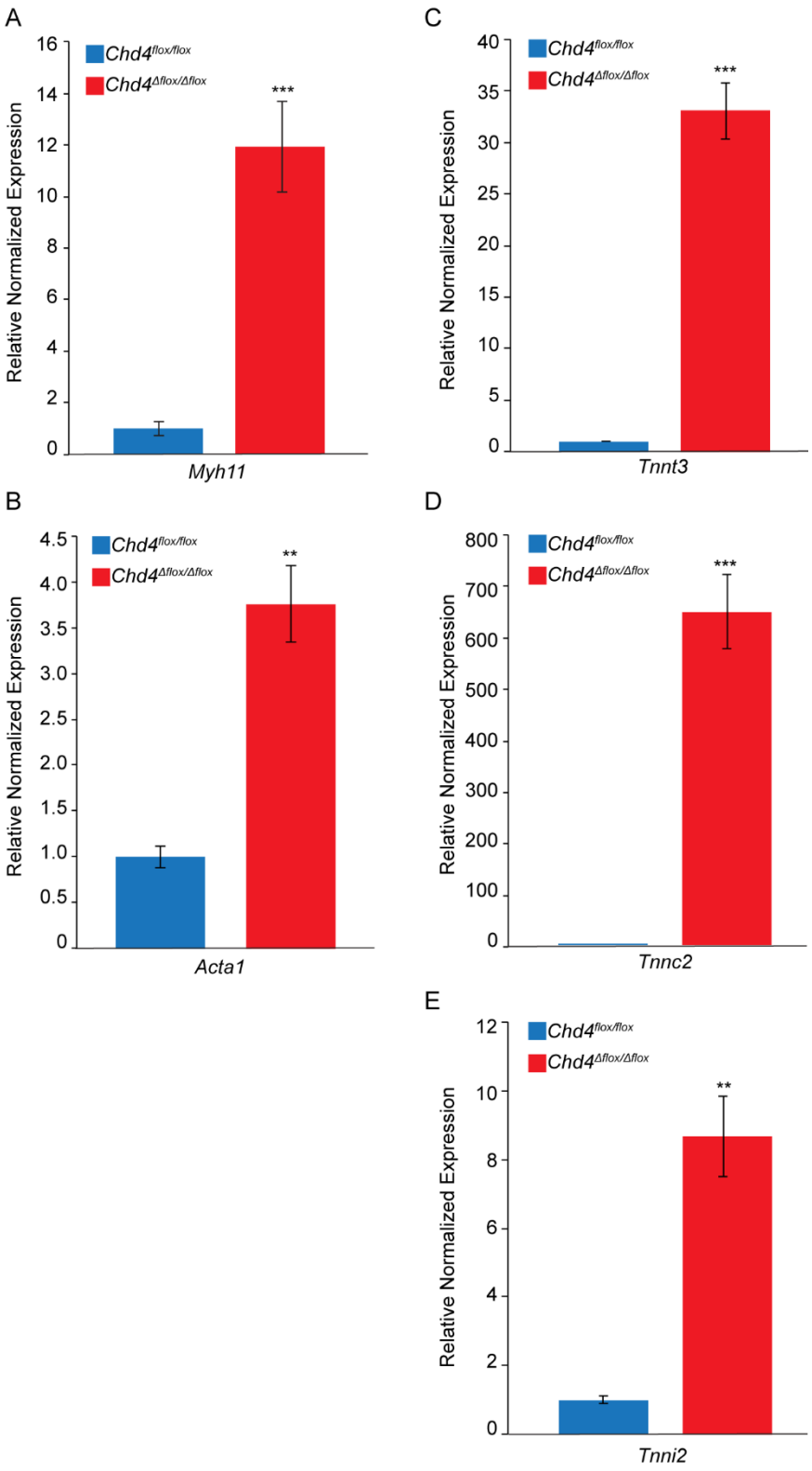

Figure S5. CHD4 is required to repress expression of non-cardiac myofibril isoforms in the embryonic heart. (A-E) Reverse transcription of RNA followed by quantitative real-time PCR (qPCR) demonstrates significantly increased expression of *Myh11* (A), *Acta1* (B), *Tnnt3* (C),

Tnnc2 (D) and *Tnni2* (E) in E10.5 $Chd4^{\Delta flox/\Delta flox}$ hearts over $Chd4^{flox/flox}$ controls by Student's t-test, ***=p-value<0.001, **=p-value<0.01, error bars represent SEM ± 0.264 and 1.763 (A), 0.122 and 0.418 (B), 0.040 and 2.731 (C), 0.319 and 71.779 (D), 0.101 and 1.172 (E). Data is represented relative to *Rps29* levels and normalized to $Chd4^{flox/flox}$ controls.

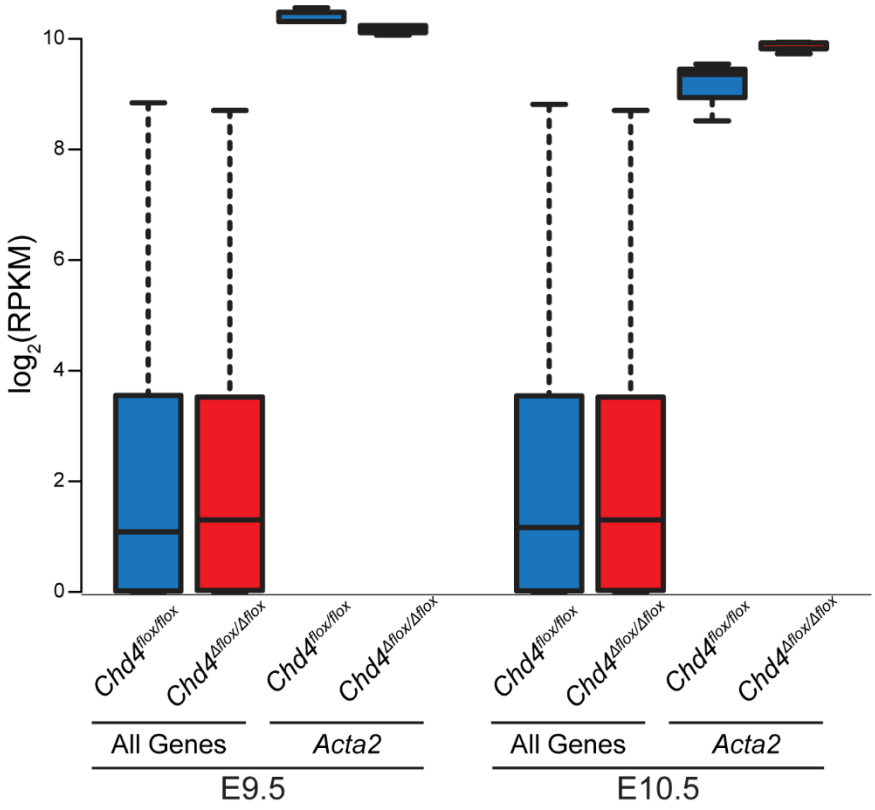

Figure S6. Acta2 is not differentially expressed in the absence of CHD4. Plotting log_2(RPKM) values from RNA-seq of *Chd4*$^{flox/flox}$ and *Chd4*$^{\Delta flox/\Delta flox}$ hearts at E9.5 and E10.5 demonstrate that *Acta2* (alpha-smooth muscle actin) is highly expressed compared to median overall gene expression but is not significantly up- or down-regulated in the absence of CHD4.

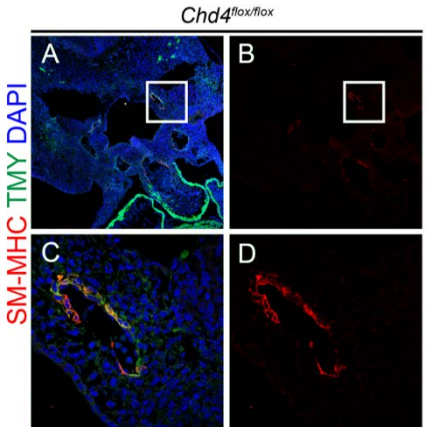

Figure S7. Smooth muscle myosin heavy chain antibody specifically stains smooth muscle cells. (A-D) Smooth muscle myosin heavy chain staining of smooth muscle cells surrounding the pharyngeal arch arteries in an E10.5 *Chd4*$^{flox/flox}$ control embryo. Boxed region denotes area of higher magnification.

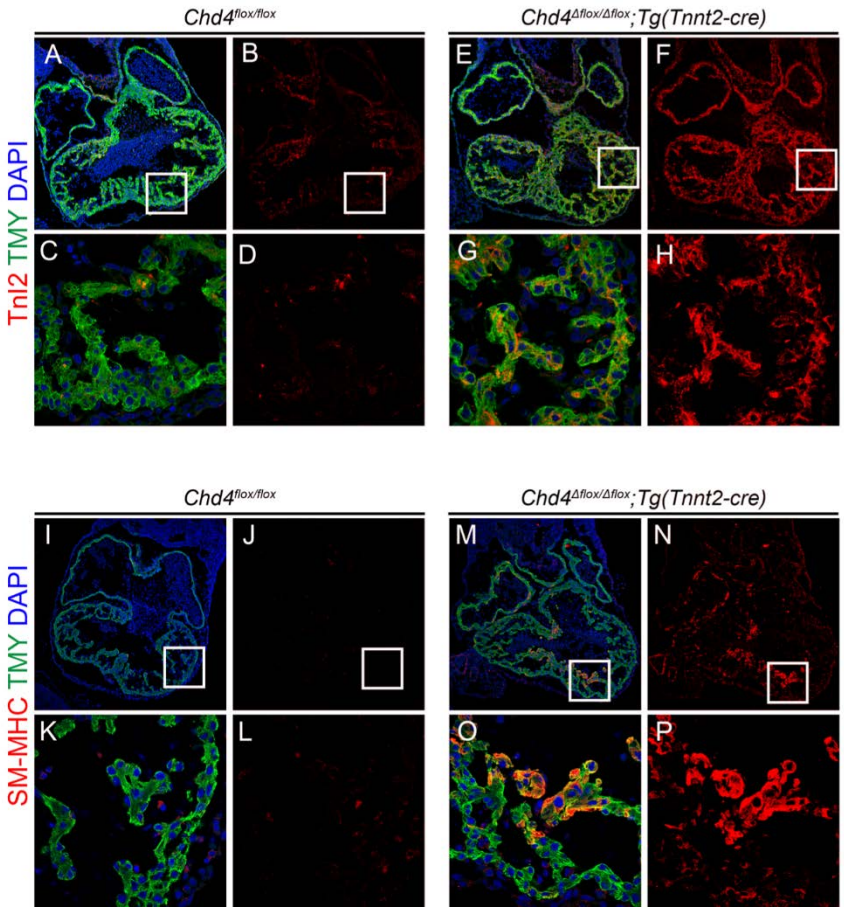

Figure S8. Ablation of CHD4 in the myocardium results in misexpression of non-cardiac myofibril paralogs. Immunohistochemistry for fast skeletal TnI2 (A-H) and smooth muscle myosin heavy chain (I-P) reveals increased expression of fast skeletal and smooth muscle myofibril subunits in the myocardium of *Chd4$^{\Delta flox/\Delta flox}$;Tg(Tnnt2-cre)* hearts (E-H, M-P) at E10.5 compared to controls (A-D, I-L). White boxes denote regions of higher magnification in adjacent panels.

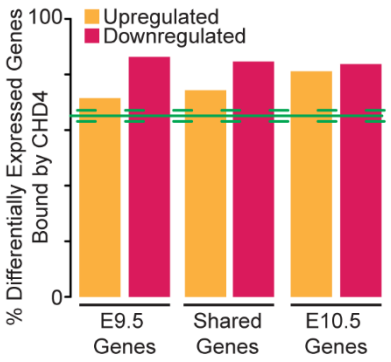

Figure S9. CHD4 directly binds genomic elements of transcriptional targets. Genes differentially expressed in *Chd4*$^{\Delta flox/\Delta flox}$ hearts at E9.5, E10.5 or commonly misregulated (shared) between both time points were cross-referenced to genes containing CHD4 ChIP-seq peaks. Columns represent the significant percentage of genes directly bound by CHD4 and either up- or down-regulated in its absence, p-value<0.001. Green solid line indicates the percent overlap expected by chance (1000 permutations) with dashed lines indicating standard deviation.

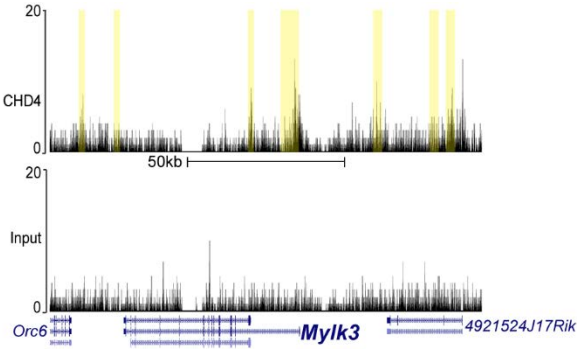

Figure S10. CHD4 binds genomic regions linked to cardiac *Mylk3*. CHD4 binding sites identified by ChIP-seq reads enriched over input DNA at cardiac myosin light chain kinase 3 (*Mylk3)* are highlighted in yellow.

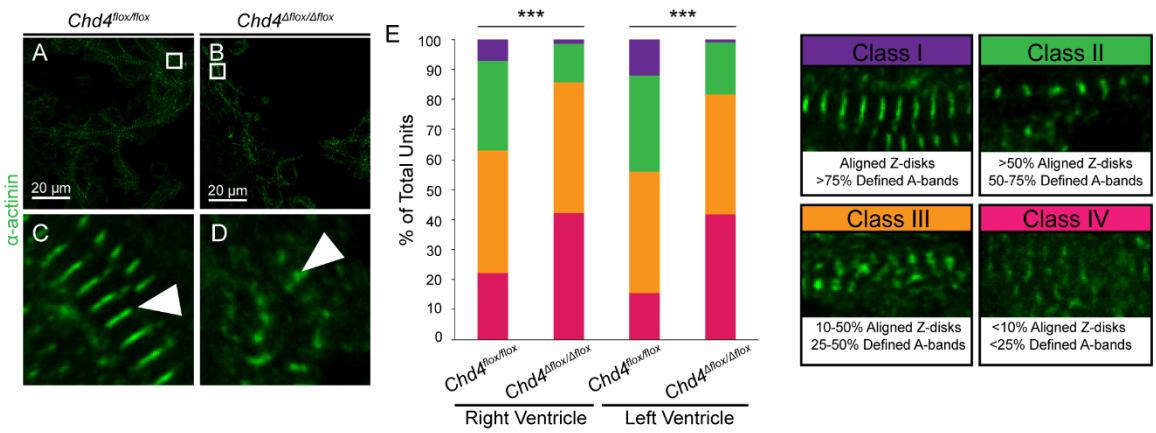

Figure S11. Misexpression of non-cardiac myofibril paralogs contribute to sarcomere disarray in the absence of CHD4. (A-D) α-actinin staining reveals disorganized sarcomere structure (wedge arrow) in *Chd4*$^{\Delta flox/\Delta flox}$ cardiomyocytes at E10.5 compared to *Chd4*$^{flox/flox}$ controls. Box denotes region of higher magnification. (E) Measurement of sarcomere organization by classification of Z-disk and A-band formation reveals significant decreases in sarcomere organization in *Chd4*$^{\Delta flox/\Delta flox}$ cardiomyocytes by χ^2 test, N= 225 vectors per ventricle per genotype, ***=p-value<0.001.

Table S1. Ablation of *Chd4* in the developing heart is embryonic lethal before E12.5.

Genotype	Stage				
	E9.5	**E10.5**	**E11.5**	**E12.5**	**P0**
***Chd4*$^{flox/flox}$**	16	33	9	19	13
	23%	**24%**	**24%**	**33%**	**27%**
***Chd4*$^{\Delta flox/\Delta flox}$**	12	29	7	3	0
	17%	**21%**	**18%**	**5%***	**0%****
***Chd4*$^{\Delta flox/+}$**	19	37	12	22	18
	27%	**27%**	**32%**	**38%**	**38%**
***Chd4*$^{flox/+}$**	24	39	10	14	17
	34%	**28%**	**26%**	**24%**	**35%**
N=	71	138	38	58	48

X^2 test, *=p-value<0.05, **=p-value<0.01

Movie S1. CHD4 is required for ventricular systolic function at E10.5. *Chd4*$^{flox/flox}$ embryo shows strong, frequent atrial and ventricular contractions measured by blood flow velocity using PW Doppler echocardiography at the atrioventricular canal.

Movie S2. Ventricular systolic function is compromised with cardiac sarcomere disarray in the absence of CHD4. *Chd4*$^{\Delta flox/\Delta flox}$ embryo has slower, weaker ventricular contractions measured by blood flow velocity using PW Doppler echocardiography at the atrioventricular canal.

References

1. Williams CJ, *et al.* (2004) The chromatin remodeler Mi-2beta is required for CD4 expression and T cell development. *Immunity* 20(6):719-733.
2. Moses KA, DeMayo F, Braun RM, Reecy JL, & Schwartz RJ (2001) Embryonic expression of an Nkx2-5/Cre gene using ROSA26 reporter mice. *Genesis (New York, N.Y. : 2000)* 31(4):176-180.
3. Dorr KM, *et al.* (2015) Casz1 is required for cardiomyocyte G1-to-S phase progression during mammalian cardiac development. *Development (Cambridge, England)*.
4. Lassmann T, Hayashizaki Y, & Daub CO (2009) TagDust--a program to eliminate artifacts from next generation sequencing data. *Bioinformatics* 25(21):2839-2840.
5. Langmead B, Trapnell C, Pop M, & Salzberg SL (2009) Ultrafast and memory-efficient alignment of short DNA sequences to the human genome. *Genome Biol* 10(3):R25.
6. Li H, *et al.* (2009) The Sequence Alignment/Map format and SAMtools. *Bioinformatics* 25(16):2078-2079.
7. Quinlan AR (2014) BEDTools: The Swiss-Army Tool for Genome Feature Analysis. *Curr Protoc Bioinformatics* 47:11.12.11-34.
8. Anders S, Pyl PT, & Huber W (2015) HTSeq--a Python framework to work with high-throughput sequencing data. *Bioinformatics* 31(2):166-169.
9. Kent WJ, *et al.* (2002) The Human Genome Browser at UCSC. *Genome research* 12(6):996-1006.
10. Love MI, Huber W, & Anders S (2014) Moderated estimation of fold change and dispersion for RNA-seq data with DESeq2. *Genome Biol* 15(12):550.
11. Mi H, Guo N, Kejariwal A, & Thomas P (2007) PANTHER version 6: protein sequence and function evolution data with expanded representation of biological pathways. *Nucleic acids research* 35:D247 - D252.
12. Shimbo T, *et al.* (2013) MBD3 localizes at promoters, gene bodies and enhancers of active genes. *PLoS genetics* 9(12):e1004028.
13. Shimbo T, Takaku M, & Wade PA (2016) High-quality ChIP-seq analysis of MBD3 in human breast cancer cells. *Genomics data* 7:173-174.
14. Schmidl C, Rendeiro AF, Sheffield NC, & Bock C (2015) ChIPmentation: fast, robust, low-input ChIP-seq for histones and transcription factors. *Nat Meth* 12(10):963-965.
15. Feng J, Liu T, & Zhang Y (2011) Using MACS to identify peaks from ChIP-Seq data. *Curr Protoc Bioinformatics* Chapter 2:Unit 2.14.
16. Shin H, Liu T, Manrai AK, & Liu XS (2009) CEAS: cis-regulatory element annotation system. *Bioinformatics* 25(19):2605-2606.

17. McLean CY, *et al.* (2010) GREAT improves functional interpretation of cis-regulatory regions. *Nature biotechnology* 28(5):495-501.
18. Reynolds ES (1963) The use of lead citrate at high pH as an electron-opaque stain in electron microscopy. *The Journal of cell biology* 17:208-212.
19. Aristizabal O, Christopher DA, Foster FS, & Turnbull DH (1998) 40-MHZ echocardiography scanner for cardiovascular assessment of mouse embryos. *Ultrasound in medicine & biology* 24(9):1407-1417.
20. Srinivasan S, *et al.* (1998) Noninvasive, in utero imaging of mouse embryonic heart development with 40-MHz echocardiography. *Circulation* 98(9):912-918.
21. Turnbull DH, Bloomfield TS, Baldwin HS, Foster FS, & Joyner AL (1995) Ultrasound backscatter microscope analysis of early mouse embryonic brain development. *Proceedings of the National Academy of Sciences of the United States of America* 92(6):2239-2243.
22. Golden HB, Sunder S, Liu Y, Peng X, & Dostal DE (2012) In utero assessment of cardiovascular function in the embryonic mouse heart using high-resolution ultrasound biomicroscopy. *Methods in molecular biology (Clifton, N.J.)* 843:245-263.

Supplemental Video 1 Still Image

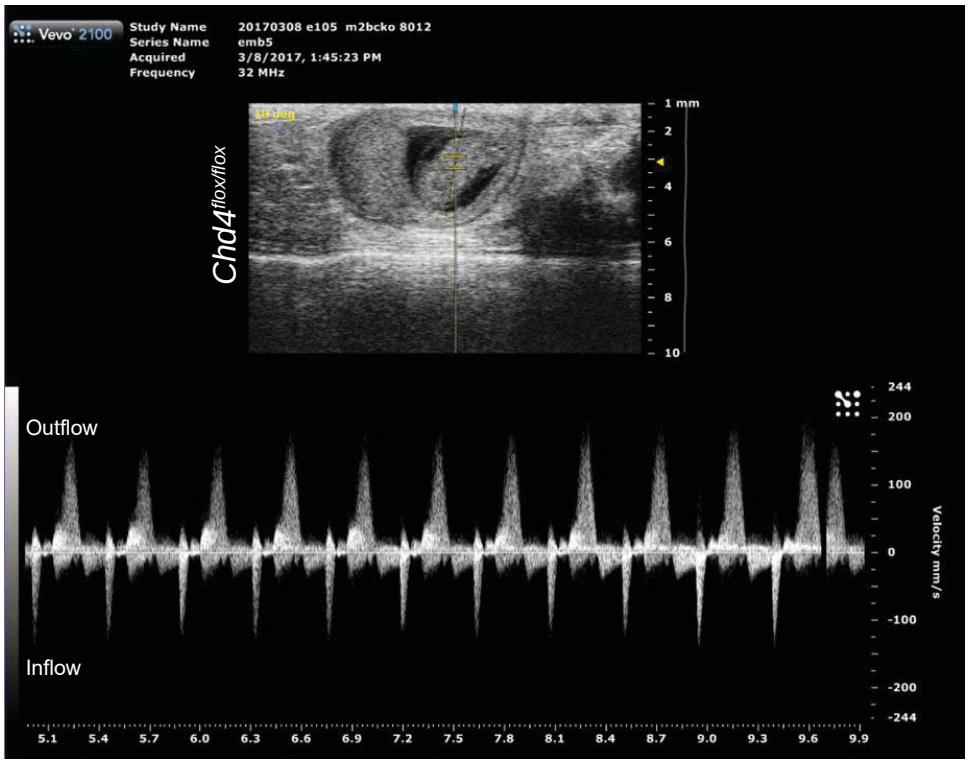

Supplemental Video 2 Still Image